

Polarization of 6- and 7-Mev Protons Elastically Scattered by Nuclei*†

ROBERT E. WARNER‡ AND W. PARKER ALFORD

Department of Physics and Astronomy, University of Rochester, Rochester, New York

(Received December 31, 1958)

Polarization measurements have been made by first scattering from the target of interest and second scattering in a carbon polarimeter for which the mean second scattering angle is 48° and for which the mean value of the polarization is greater than $+70\%$ for $5 \text{ Mev} \leq E_2 \leq 6 \text{ Mev}$. The polarization as a function of angle at 15° intervals from 45° to 135° is reported near 6 Mev for Al, Ti, V, Cr, Fe, Co, Ni, Cu, and Zn, and near 7 Mev for Al, Fe, Ni, and Cu. $P(\theta)$ usually shows an oscillatory behavior, with the magnitude of the maxima and minima never greater than about 40%. The polarization as a function of energy is reported for C at 45° from 5.7 to 6.8 Mev, and for Fe and Cu at 60° and 120° from 5.8 to 6.4 Mev. For C, $P(45^\circ)$ decreases from $+92\%$ at 5.7 Mev to $+36\%$ at 6.8 Mev. For Cu, $P(60^\circ)$ and $P(120^\circ)$ vary slowly, if at all, with energy, but a rapid energy variation for Fe is observed, possibly due to resonance effects in compound elastic scattering.

INTRODUCTION

IN recent years there has been much interest in the polarization of nucleons elastically scattered by complex nuclei. Until about 1956 most proton polarization measurements had been made at energies from about 100 to 400 Mev.¹ More recently such work has been extended to 18 Mev² and to 10 Mev.³ Neutron polarization measurements have been made at 3 Mev⁴ and at 1 Mev and lower.⁵

The optical model of the nucleus⁶ has been used to calculate both angular distributions⁷⁻⁹ and polarizations^{9,10} in elastic nucleon-nucleus scattering. Precise proton angular distribution data are now available for V, Cr, Fe, and Co from about 4 to 7 Mev.¹¹ It was hoped that proton polarization measurements at about 6 and 7 Mev on nuclei from $Z=13$ to 30 might provide information about the strength of the spin-orbit coupling between protons and complex nuclei. The polarization data, in conjunction with the angular distribution data, should enable one to determine

whether an optical model can fit both sets of data with the same set of parameters.

APPARATUS

The source of protons for these experiments was the Rochester 27-in. variable energy cyclotron, shown in Fig. 1. The cyclotron beam extraction system consists of an electrostatic deflector followed by an iron pipe and a pair of quadrupole magnets which focus the beam through a slit. The beam then enters a double focusing wedge analyzing magnet which focuses a monoenergetic beam into either of two scattering chambers. At the beginning of a run the beam was focused into the 10-in. scattering chamber and the analyzing magnet field measured by proton resonance. An energy calibration of the magnet has been made with natural alpha emitters and by (p,n) threshold measurements, hence the proton energy could be obtained from the field strength.

To obtain a larger beam intensity the actual polarization measurements were made in a pair of scattering chambers (not shown in Fig. 1) just in front of the analyzing magnet. Beam currents from 0.2 to 1.0 microamperes were employed in most runs. Although the deflector voltage and condensing magnet current

* Supported by the U. S. Atomic Energy Commission and the Esso Educational Foundation.

† Based on a thesis submitted to the Graduate School of the University of Rochester in partial fulfillment of requirements for the degree Doctor of Philosophy.

‡ National Science Foundation Predoctoral Fellow.

¹ For a comprehensive bibliography see L. Wolfenstein, in *Annual Review of Nuclear Science* (Annual Reviews, Inc., Palo Alto, 1956), Vol. 6, p. 43.

² K. W. Brockman, Jr., *Phys. Rev.* **110**, 163 (1958); W. Blanpied, *Phys. Rev.* **113**, 1099 (1959).

³ L. Rosen, *Proceedings of the Second United Nations International Conference on the Peaceful Uses of Atomic Energy, Geneva, 1958* (United Nations, Geneva, 1959).

⁴ McCormac, Steuer, Bond, and Hereford, *Phys. Rev.* **108**, 116 (1957).

⁵ S. E. Darden, *Proceedings of the University of Pittsburgh Conference on Nuclear Structure, June, 1957*, edited by S. Meshkov (University of Pittsburgh and Office of Ordnance Research, U. S. Army, 1957).

⁶ Feshbach, Porter, and Weisskopf, *Phys. Rev.* **96**, 448 (1954).

⁷ A. E. Glassgold and P. J. Kellogg, *Phys. Rev.* **107**, 1372 (1957).

⁸ Melkanoff, Nodvik, Saxon, and Woods, *Phys. Rev.* **106**, 793 (1957).

⁹ Culler, Fernbach, and Sherman, *Phys. Rev.* **101**, 1047 (1956).

¹⁰ Campbell, Bjorklund, and Fernbach (private communication).

¹¹ C. A. Preskitt and W. P. Alford, Atomic Energy Commission Report NYO-2172 (unpublished).

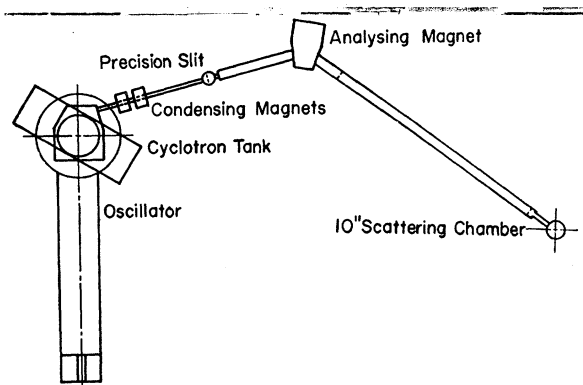


FIG. 1. Plan view of Rochester 27 in. variable energy cyclotron.

required small adjustments during a run, it was found that these adjustments varied the beam energy less than $\pm\frac{1}{2}\%$ from its mean value. To avoid bringing the beam out through the analyzing magnet each time the energy was changed, the energy was sometimes determined by measuring the cyclotron oscillator frequency, which is known to be proportional to the square root of the energy of the analyzed beam within the error of determining the beam energy.

Although helium has been used as the analyzer in previous low-energy proton polarization measurements,^{12,13} it has been found^{2,14} that for appropriate ranges of energy and scattering angle carbon may be used as an analyzer. Carbon was chosen for the present work because of the larger counting rates and improved resolution of signal from background which could thereby be obtained. A proton beam with an energy spread of about 100 keV and a mean energy in the range 6 to 7 MeV was elastically scattered from elemental targets of Al, Ti, V, Cr, Fe, Co, Ni, Cu, and Zn. The scattered beam was second scattered from the carbon nuclei in a polystyrene foil. Events in which the second scattering was from a proton in the polystyrene were rejected by pulse-height analysis.

All first scatterings were to the right of the incident beam, hence the polarization $P_1(E_1, \theta_1)$ is given by¹⁵

$$P_1(E_1, \theta_1) \bar{P}_2(\bar{E}_2) = (R - L) / (R + L). \quad (1)$$

R and L are the second scattering intensities in the plane of first scattering to the right and left, respectively, of the first scattered beam. $\bar{P}_2(\bar{E}_2)$ is the known polarization produced in scattering from carbon at the mean energy \bar{E}_2 averaged over the acceptance angles of the detectors and over the energies of second scattering.

The first scattering chamber, shown with polarimeter attached in Fig. 2, consists of three separable sections.

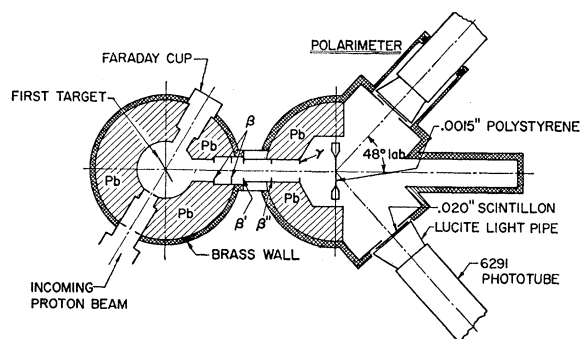


FIG. 2. First scattering chamber and carbon polarimeter for polarization experiments. Aperture α defines the incident beam. Apertures β , β' , β'' , and γ collimate the first scattered beam.

¹² J. C. Hensel and W. C. Parkinson, Phys. Rev. **110**, 128 (1958).

¹³ M. J. Scott, Phys. Rev. **110**, 1398 (1958).

¹⁴ R. E. Warner and W. P. Alford, Atomic Energy Commission Report NYO-8576 (unpublished).

¹⁵ J. V. Lepore, Phys. Rev. **79**, 137 (1950).

The bottom section is permanently bolted to a $\frac{3}{8}$ -in. aluminum base plate. The entrance slit α , $\frac{3}{32}$ in. \times $\frac{1}{4}$ in. through 0.010-in. Ta, limits the beam striking the first target. It and a target holder (not shown) are positioned on the bottom section with aligning pins. The center section contains 5 ports into which the polarimeter may be inserted, and may be rotated to allow first scattering at angles from 45° to 135° at 15° intervals. An exit port on the center section carries a Faraday cup for beam integration. An aligning pin maintains the correct orientation of the center section relative to the bottom section. The target is attached to a shaft inserted through the top section, and an angular scale on top of this section indicates the orientation of the target relative to the incident beam.

The second scattering chamber (or polarimeter), shown in Fig. 2, is positioned at one end by a port of the first scattering chamber, and at the other end by an arm which rotates about the vertical axis of the first scattering chamber. The target holder contains a 0.0015-in. polystyrene foil which is held normal to the first scattered beam and may be lifted out of the beam for background measurements. The foil may be rotated through 180° to eliminate spurious asymmetries from target nonuniformities. $\frac{7}{8}$ -in. \times $1\frac{1}{2}$ -in. apertures through 0.010-in. brass subtending 0.16 steradian at a mean laboratory angle of 48° define the second scattered particles, which are detected by scintillation crystals $\frac{1}{8}$ in. \times $1\frac{3}{8}$ in. \times 0.020 in. The crystals will just stop 6-MeV protons. The left and right scintillation crystals give energy resolutions of 11 and 16%, respectively, for 5-MeV protons. The crystals are covered with 0.3-mil aluminum foil to improve the pulse height and resolution. Lucite light pipes convey the light from the crystals to 6291 photomultiplier tubes, the three units being permanently bonded together.

The apertures which define the first scattered beam are also shown in Fig. 2. The four apertures β , β' , and β'' prevent protons scattered from the walls from reaching either the detectors or the second target. The two apertures β are $\frac{1}{2}$ -in. D through 0.005-in. tantalum, and are supported by an annular piece of lead in the first scattering chamber which also attenuates γ radiation originating in the first target. The two apertures β' and β'' are through 0.010-in. brass and are inserted in the entrance port of the polarimeter. The aperture γ , also through 0.010-in. brass, limits the first scattered beam striking the second target. Originally β' , β'' , and γ were $\frac{1}{32}$ in., $\frac{1}{2}$ in., and $\frac{1}{2}$ in. in diameter, respectively; later they were expanded to $\frac{1}{16}$ in., $\frac{9}{16}$ in., and $\frac{3}{8}$ in. to give larger counting rates. Other shielding, not shown, included an 18-in. concrete wall and 4 in. of lead between the detectors and the cyclotron tank.

Pulses from the phototubes were amplified with Los Alamos Model 500 amplifiers and recorded with two pulse-height analyzers, one an RIDL one-hundred channel analyzer and the other a sixteen-channel analyzer built at this laboratory. An Atomic Instrument

Company Model 101-M Discriminator was connected in parallel with each pulse-height analyzer, and these discriminators were set to count all pulses above the bottom of the elastic peak of the second scattered protons. At the end of a run the number of counts in the elastic peak was also obtained from the pulse-height spectra, and this number was compared with the discriminator count. If the two numbers were equal it was inferred that the electronic circuits were functioning properly. The pulse-height analyzers were occasionally interchanged to insure that they had no systematic effects on the counting rates: none were found in normal operation. Dead times (5 μ sec for the discriminators) were short enough to introduce negligible error in all experiments.

It is necessary that any instrumental effects tending to cause spurious right-left asymmetries be either eliminated or well understood. One such effect would be a failure of the polarimeter axis to intersect the center of the beam spot on the first target. To prevent this, before beginning the experiments a pointed mandril was inserted in the polarimeter entrance port and, at a given θ_1 , made to point to the center of rotation of the first target. Permanent reference marks were then made to enable one to correctly position the polarimeter support arm for each θ_1 . It was then attempted to align aperture α so that the beam going through it was centered at the center of rotation of the first target. This was done imperfectly; however one could measure and correct for the resulting misalignment as described later. Aside from this, asymmetries due to misalignment of the polarimeter axis could not exceed ± 0.005 . Asymmetries caused by wrinkling and nonuniform target thickness were eliminated by turning both targets through 180° halfway through each run.

One must allow for the possibility that the two scintillation detectors will have different efficiencies, resulting from slightly different defining aperture areas or angular positions. This was investigated by observing

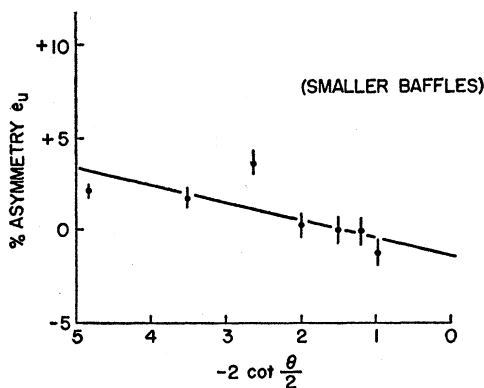


FIG. 3. Asymmetry due to finite geometry with unpolarized first scattered beam. First target is platinum, and the second is nickel. Straight line has slope calculated from geometry of apparatus and differential cross sections.

the left and right counting rates for a given first scattering process with the polarimeter in both its normal and inverted (i.e., turned 180° about its axis) positions. Calling E_L and E_R the efficiencies of the left and right counters, respectively, E_L/E_R was found equal to 0.992 ± 0.005 for the smaller set of apertures (β' , β'' , γ) and 1.020 ± 0.005 for the larger set. The difference is attributed to a slightly eccentric aperture in the larger aperture γ .

Even when the first scattered beam is unpolarized, a left-right asymmetry will, in general, be observed because of the variation of the first differential scattering cross section over the range of angles accepted by the aperture γ . If we call the counting rates for an unpolarized first scattering L_u and R_u , the asymmetry is calculated to be

$$e_u = \frac{L_u - R_u}{L_u + R_u} = a \frac{\sigma_1'}{\sigma_1} \left(\frac{\sigma_2'}{\sigma_2} - 1.31 \right), \quad (2)$$

$$a = 2.60 \times 10^{-3} \quad (\text{larger apertures}) \\ = 1.66 \times 10^{-3} \quad (\text{smaller apertures}).$$

σ_i and σ_i' are the differential cross section and its first derivative with respect to θ for scattering from the i th target.

The above prediction was tested experimentally for the smaller apertures with a platinum first target and a nickel second target. The scattering from platinum is Rutherford, hence $\sigma_1'/\sigma_1 = -2 \cot(\theta/2)$. The observed asymmetries are plotted against $\cot(\theta/2)$ in Fig. 3. The slope of the straight line is that predicted by the above equation. However, it does not go through zero when $\cot(\theta/2) = 0$. This is attributed to a small permanent misalignment of aperture α , and this is compensated by adding -0.013 to all observed asymmetries. These data also reveal a permanent misalignment of the polarimeter for $\theta_1 = 75^\circ$, and a correction of $+0.017$ is made for all data taken at this angle. Otherwise the data scatter from the theoretical prediction by about $\pm 1\%$. This is attributed to the motion of the beam spot over the beam defining aperture α , and an extra 1% probable error has been added to the final data to allow for this. A similar test of the finite geometry effect was made for the larger apertures, with equally satisfactory results.

If the counting rates for a polarized first scattering are L_P and R_P , it is easily shown that:

$$P_1 \bar{P}_2 (1 + \rho e_u) = \rho + e_u, \quad \rho = (R_P - L_P) / (R_P + L_P). \quad (3)$$

For all experiments presently described $|\rho e_u| \leq 0.01$, and therefore all polarizations were computed with $(1 + \rho e_u)$ set equal to unity. The error thus introduced is much less than that arising from the uncertainty in \bar{P}_2 .

The polarization of protons elastically scattered from carbon at angles near 48° was calculated from the phase shifts for $C^{12}(p, p)C^{12}$, which are known to about

5 Mev.¹⁶ This polarization changes very rapidly with energy near 4.8 Mev because of a resonance at that energy, hence it was necessary to do all second scattering above about 4.9 Mev. Since the phase shifts were not known above 5 Mev, $\bar{P}_2(\bar{E}_2)$ was determined experimentally as follows. By using a helium polarimeter¹⁷ formerly in use at this laboratory it was determined that protons scattered from carbon at 5.8 Mev and 45° have a polarization of $+0.92 \pm 0.09$.¹⁸ The carbon polarimeter was then placed in position at $\theta_1 = 45^\circ$ with a carbon first target. With the incident energy again 5.8 Mev, the mean energy at second scattering was 5.15 Mev, and $P_2(5.15 \text{ Mev})$ was thus determined.

The calibration was extended to higher energies as follows. First a double scattering experiment at a first scattering energy E greater than 5.8 Mev was performed. The first scattered beam was degraded to such an energy that $\bar{P}_2(\bar{E}_2)$ was known, and thus $P_1(E, 45^\circ)$ was determined. Then the absorber was removed from the first scattered beam and, with no other changes, the experiment was repeated; thus $\bar{P}_2(\bar{E}_2)$ was determined for a higher \bar{E}_2 than had been reached previously. By repeating this two-step process several times the calibration curve shown in Fig. 4 was obtained. The dashed curves indicate the experimental error assigned to the calibration. The data $P_1(E, 45^\circ)$ are also shown.

EXPERIMENTAL PROCEDURE AND DATA ANALYSIS

The first targets used were 70 kev to 190 kev thick to 6-Mev protons. Near the end of the work the spectra of 6-Mev protons first scattered from all targets was investigated with 5% resolution. In all cases either an upper limit of 1% could be set on carbon-oxygen contamination, or such contamination was negligible compared to inelastic events in the same energy range. Heavy element contamination was specified to be less than 1% for the commercially-obtained targets. In preparing other targets in this laboratory only chemically pure reagents were used in the electropolishing and electroplating solutions, therefore these targets are believed to be equally free from such contamination.

For the angular distributions near 6 Mev, the first target was placed so that the normal to it bisected the scattering angle. At the time these measurements were made it was not realized that the polarimeter was effective up to 6 Mev, and it was thus desired to minimize the spread of second-scattering energies. Consequently the range of first-scattering energies for these data increases with increasing angle, and the

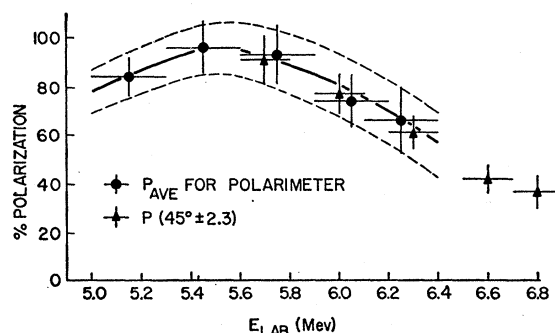


FIG. 4. Mean polarization of carbon polarimeter as a function of mean second scattering energy. The solid curve is the value of \bar{P}_2 used, and the dashed curves indicate the probable error. Also shown are $P(45^\circ \pm 2.3^\circ)$ as a function of energy for carbon.

probable error in the energies quoted for these data is half the maximum target thickness presented to the beam. For the angular distributions near 7 Mev and for the energy variation on Fe and Cu at 60° and 120° , the first target was set in one of the two positions at an angle of 60° to the beam, the transmission position being used for θ_1 between 45° and 90° , and the reflection position otherwise. Thus for the angular distributions near 7 Mev the range of first scattering energies is the same for all data, except for the energy fluctuations of $\pm 0.5\%$ due to variations in the cyclotron oscillator frequency.

The energy of second scattering was kept within the calibration range of the polarimeter by placing aluminum absorbers in the first scattered beam, if necessary. This absorber decreases the energy of the protons without affecting their polarization.¹⁹

In each run, with both targets in position, the first target was exposed to the cyclotron beam, several hundred microcoulombs of charge being a typical exposure. Then, with the second target lifted out of the first scattered beam, an appropriate background exposure was made. Finally, both targets were turned through 180° and both previous exposures repeated. Moving the second target is expected to change the background slightly since, for example, neutrons can scatter from nuclei in the second target. By experiments in which background was determined first in the usual manner and second by stopping the first scattered protons with absorber, it was found that such effects introduce negligible experimental error.

To compute e_u in Eq. (2), σ_2'/σ_2 was calculated from the $C^{12}(p,p)C^{12}$ angular distribution data of Schneider.²⁰ The values thus obtained were confirmed experimentally by first scattering from Pt at 45° , and second scattering from carbon. σ_1'/σ_1 was obtained from Preskitt's data¹¹ for V, Cr, Fe, and Co, and from Schneider's data²¹ for Cu. For Al Rutherford angular dependence was

¹⁶ Reich, Russell, and Phillips, Phys. Rev. 104, 143 (1956).

¹⁷ W. P. Alford and R. E. Warner, Atomic Energy Commission Report NYO-2174 (unpublished). The helium polarimeter has $\theta_{2, lab} = 118^\circ$, $E_2 = 4.5$ to 5 Mev, and $\bar{P}_2 = -0.85 \pm 0.05$.

¹⁸ P is taken to be positive in the direction $\mathbf{k}_j \times \mathbf{k}_i$, where \mathbf{k}_j and \mathbf{k}_i are the propagation vectors of the scattered and incident waves, respectively.

¹⁹ L. Wolfenstein, Phys. Rev. 75, 1664 (1949).

²⁰ H. Schneider, Helv. Phys. Acta. 29, 55 (1956).

²¹ H. Schneider *et al.*, Helv. Phys. Acta 27, 170 (1954).

assumed. For Ni and Zn Preskitt's iron data were assumed to be usable, and his Cr data were applied to Ti. It is estimated that these assumptions for Al, Ni, Zn, and Ti will give rise to rms errors of about ± 0.005 in the polarization data. If future precision differential cross section measurements are made for these elements, such data could be used to correct the present polarization data.

The net counting rates were corrected for detector efficiency as described previously. The gain of both detectors was stable to about 1% over a period of several hours, therefore the statistical errors in both counting rates were increased to include the probable errors arising from drifts of this magnitude. Finally, we allowed for the possibility of a contamination of inelastic events as follows. An upper limit on the number of inelastic events counted was obtained by examining the shape of the pulse-height spectra. Calling this number and its associated probable error A and a , respectively, it was found that A was always comparable with a . Hence no subtraction was ever made from the net count, but the square of its probable error was increased by the square of the larger of A and a . This correction never increased the probable error to more than 1.4 times its original value. After all these corrections were applied, the polarization was computed from Eq. (3) and Fig. 4.

The probable error in the polarization thus includes, in addition to counting statistics, the uncertainty in the detector efficiency ratio, geometric corrections, possible inelastic contamination, polarimeter calibration, and electronics drifts. The ports on the first scattering chamber are positioned correctly to 0.5° , and a probable error of $\pm 2.3^\circ$, the angular definition of aperture γ , is assigned to the first scattering angle. Since the cyclotron oscillator frequency was found to remain constant within $\pm 0.3\%$ over several days, a probable error of half the target thickness plus 0.6% of the beam energy was assigned to the first scattering energy.

RESULTS AND CONCLUSIONS

The data obtained are given in Figs. 5 through 7. The curves in Figs. 5 and 6 represent unpublished optical model calculations by G. Campbell, F. Bjorklund, and S. Fernbach, who used a Coulomb potential for a nucleus of uniform charge density plus a nuclear potential given by:

$$V = U_0 \rho(r) + iV_0 \exp[-(r-R_0)^2/b^2] \\ + \lambda U_0 \left(\frac{\hbar}{\mu c} \right)^2 \frac{d\rho(r)}{r dr} \sigma \cdot L,$$

$$\rho(r) = [1 + \exp\{(r-R_0)/a\}]^{-1}, \quad R_0 = r_0 A^{1/3},$$

with the parameters $U_0 = 50-56$ Mev, $V_0 = 5-9$ Mev, $\lambda = 40$, $a = 0.65f$, $b = 1.2-1.5f$, $r_0 = 1.25f$. These parame-

ters, which are close to those used to fit the 4- to 14-Mev neutron scattering data,²² were chosen to fit the present data. The theoretical curves have been corrected for an estimated amount of compound elastic scattering: in making this correction it was assumed that the compound elastic scattering was isotropic and unpolarized, and differential cross sections of about 8 mb/sterad and 20 mb/sterad for odd and even elements were estimated from Preskitt's¹¹ data.

Figure 5 shows $P(\theta)$ near 6 Mev for all nine targets previously listed; the neutron background from vanadium was so severe that measurements could not be extended beyond 75° . Most of these elements show maxima at 60° to 75° , while for Al there is a maximum

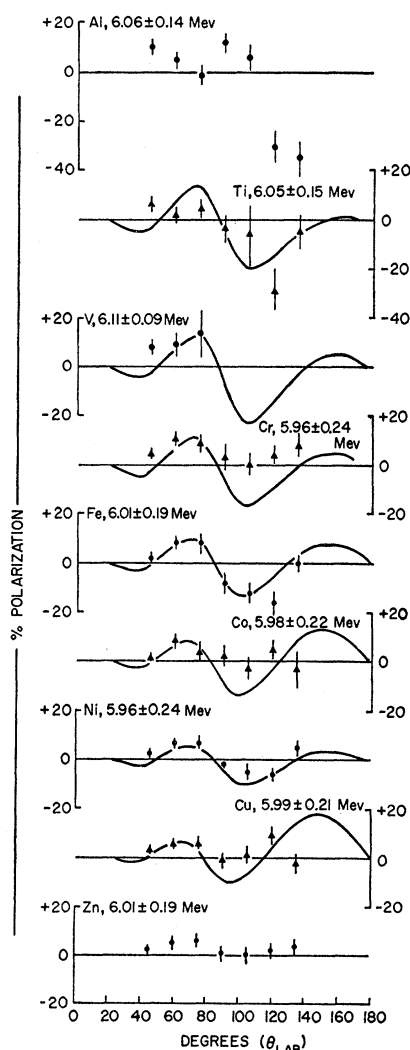


FIG. 5. Polarization as a function of angle for 6-Mev protons elastically scattered from various nuclei. Polarization is in percent, and energies and angles are in the laboratory system. Curves represent calculations of Campbell *et al.*, corrected for compound elastic scattering.

²² F. Bjorklund and S. Fernbach, Phys. Rev. **109**, 1295 (1958).

at 45° . At back angles the data vary more erratically from element to element.

At 6 Mev the optical model calculations usually fit the forward polarization maxima which appear in these experiments. At back angles, where the polarization varies erratically from element to element, it is clear that all data will not be fitted by a single set of parameters and in fact the theoretical calculations are not in good agreement with the data. However other calculations (not shown) by Campbell *et al.* show that the calculated polarizations are quite sensitive to small changes in the optical model parameters, and thus it might be possible to fit the data for each target nucleus separately. Such a procedure might not be unreasonable since one expects structural effects to be significant at these energies. More specifically, it was found that increasing b made the calculated $P(\theta)$ oscillate more

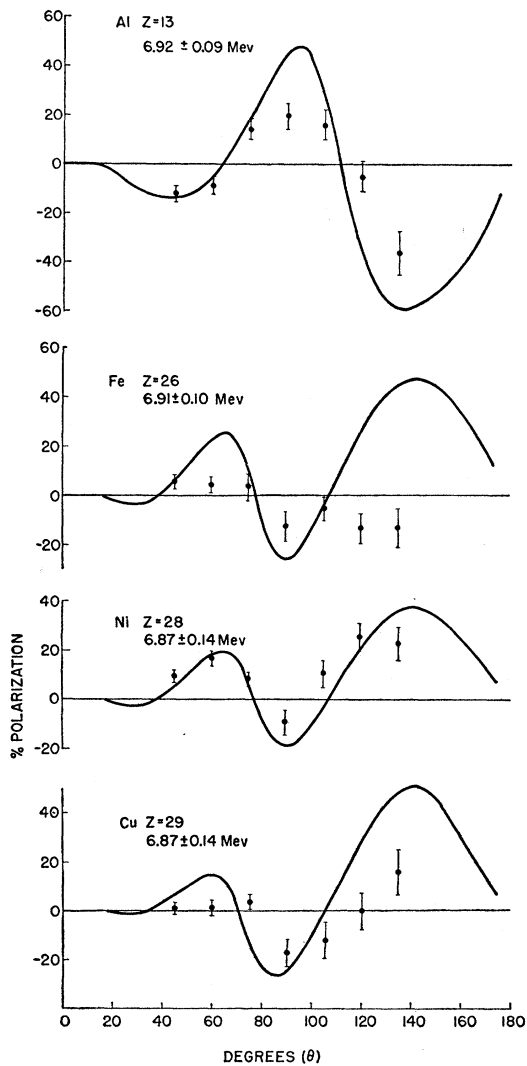
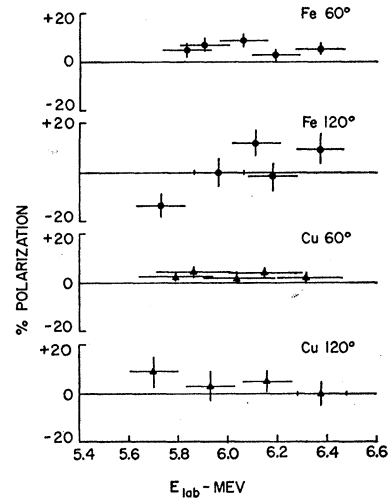


FIG. 6. Polarization as a function of angle for 7-Mev protons. Polarization is in percent, energies and angles are in the laboratory system.

FIG. 7. Polarization as a function of energy for protons scattered from Fe and Cu at 60° and 120° .



rapidly, and one would thus expect that to fit the 6-Mev data for Ni would require a smaller b than for Cu. This seems reasonable from the standpoint of the shell model, since Cu contains more nucleons outside the closed $f_{7/2}$ shells and consequently is expected to have a more diffuse surface. This argument appears to break down when applied to the 7-Mev Ni and Cu data since these data show about the same angular dependence; however the importance of these shell-model effects should change with energy. Such effects appear to vanish near 10 Mev, since the 10 Mev³ and 17 Mev² data vary much more smoothly with A than do the present data.

The 7-Mev data for Al, Fe, Ni, and Cu are shown in Fig. 6. The calculations for Ni and Al fit the data rather well except that the amplitude for Al is slightly too large, indicating that a smaller λ should have been used for Al. The calculations give about the right angular dependence for Cu except at 60° . The Fe calculations bear little resemblance to the data, and at 120° and 135° have the wrong sign. This may indicate that the compound elastic scattering is polarized.

It appears that, for a given element, the polarization tends to increase as the bombarding energy is increased. At 6 Mev, the largest polarizations at back angles are for Al and Ti (but not Cr), indicating a tendency for the polarization to increase with decreasing A at fixed energy. Both these effects indicate that the polarization increases as the bombarding energy is raised relative to the Coulomb barrier height.

Data for the polarization as a function of energy for Fe and Cu at 60° and 120° are given in Fig. 7. The Cu data indicate a smooth variation of P between the values observed at 6 and 7 Mev. The Fe data, particularly at 120° , display a more erratic energy variation which may be related to resonance effects in compound elastic scattering. Preskitt¹¹ also presents evidence that compound elastic scattering from iron may be important

at these energies: he finds that the ratio of the elastic scattering cross section to the Rutherford cross section varies more rapidly at back angles for Fe than for the odd elements V and Co, for which compound elastic scattering is considerably weaker as a result of the lower (p,n) thresholds. However earlier Ni polarization data¹⁷ at 5.7 Mev are very close to the present 6-Mev Ni data. If compound elastic scattering causes the rapid energy variation for Fe, one would expect a similar effect for Ni.

In conclusion, the present work indicates that optical model parameters which fit other experimental data in this energy region give a qualitative description of the polarization, but detailed agreement is not obtained with a single set of parameters. The failure to obtain a detailed fit may result from a finite contribution to the polarization from the compound elastic scattering despite the fact that our target thicknesses imply an average over many compound levels. Such a breakdown of the usual statistical assumption referring to the contribution from compound levels can, for example, come from the preponderance of compound levels of a particular spin and parity among those levels which could be important at the excitation energy under consideration. The work of Schiffer *et al.*²³ on the

$\text{Ni}^{58}(p,p'\gamma)\text{Ni}^{58}$ reaction suggests that over a range of bombarding energies of about 100 kev most of the strongly excited levels may have the same spin and parity. On the other hand, the possibility has not yet been fully explored that the fit to the polarization data could be greatly improved by small variations of the parameters a , b , V_0 , and λ which relate to the surface of a given nucleus. If successful, this latter idea could make the polarization data a useful tool for providing information about the nuclear surface.

ACKNOWLEDGMENTS

The authors are especially indebted to Professor Erich Vogt for his critical reading of this manuscript and for several stimulating discussions in regard to the theoretical significance of the work, and to Dr. G. Campbell, Dr. F. Bjorklund, and Dr. S. Fernbach of Livermore for sending us their calculations in advance of publication. Dr. F. Seward supplied several targets and made helpful suggestions regarding the operation of the cyclotron. R. Hawrylak, A. Hamann, and S. Oakes rendered valuable technical assistance, and Mr. E. Griffin operated the cyclotron during some of the measurements.

²³ Schiffer, Moore, and Class, Phys. Rev. **104**, 1661 (1956).